Multiscaling fractional advection-dispersion equations and their solutions

Rina Schumer and David A. Benson

Desert Research Institute, Reno, Nevada, USA

Mark M. Meerschaert

Department of Mathematics, University of Nevada, Reno, Nevada, USA

Boris Baeumer

Department of Mathematics and Statistics, University of Otago, Dunedin, New Zealand

[1]   The multiscaling fractional advection-dispersion equation (ADE) is a multidimensional model of solute transport that encompasses linear advection, Fickian dispersion, and super-Fickian dispersion. The super-Fickian term in these equations has a fractional derivative of matrix order that describes unique plume scaling rates in different directions. The directions need not be orthogonal, so the model can be applied to irregular, noncontinuum fracture networks. The statistical model underlying multiscaling fractional dispersion is a continuous time random walk (CTRW) in which particles have arbitrary jump length distributions and finite mean waiting time distributions. The meaning of the parameters in a compound Poisson process, a subset of CTRWs, is used to develop a physical interpretation of the equation variables. The Green's function solutions are the densities of operator stable probability distributions, the limit distributions of normalized sums of independent, and identically distributed random vectors. These densities can be skewed, heavy-tailed, and scale nonlinearly, resembling solute plumes in granular aquifers. They can also have fingers in any direction, resembling transport along discrete pathways such as fractures.   *INDEX TERMS:* 1832 Hydrology: Groundwater transport; 1869 Hydrology: Stochastic processes; 3250 Mathematical Geophysics: Fractals and multifractals; 5104 Physical Properties of Rocks: Fracture and flow; 5139 Physical Properties of Rocks: Transport properties; *KEYWORDS:* fractional, dispersion, fractal, fracture, anomalous, transport

1. Introduction

[2]   Hundreds of studies have proposed modeling techniques to address the super-Fickian transport of solutes in aquifers. Among them are fractional advection-dispersion equations (ADEs), analytical equations that employ fractional derivatives in describing the growth and scaling of diffusion-like plume spreading. Fractional ADEs are the limiting equations governing continuous time random walks (CTRW) with arbitrary particle jump length distribution and finite mean waiting time distribution [*Compte*, 1996]. They are a subset of fractional kinetic equations that allow fractional derivatives in both the space and time operators [*Saichev and Zaslavsky*, 1997; *Benson*, 1998; *Mainardi et al.*, 2001]. The spatially fractional equations are particularly suited to application in hydrogeology because they have tractable Green's function solutions, given by stable probability distributions.

[3]   One-dimensional fractional ADEs have been used to model the heavy leading edges and nonlinear scaling of conservative plumes observed in both laboratory and field solute transport experiments [*Benson*, 1998; *Pachepsky et al.*, 2000; *Benson et al.*, 2001]. These phenomena were reproduced without the addition of scale-dependent parameters or the use of high-resolution numerical simulations. The dispersion coefficient in each experiment was constant over time, since the spatially fractional derivatives account for the nonlinear link between plume size and time (t).

[4]   In a Fickian plume, the dispersion coefficient is larger in the longitudinal direction than in the transverse directions, but the scaling rate is constant and growth is proportional to $t^{1/2}$ in all directions [*de Josselin de Jong*, 1958]. *Meerschaert et al.* [2001] demonstrate that a contaminant plume can also have different scaling rates in various directions (Figure 1). They derive a multiscaling fractional ADE in which unique fractional derivatives govern scaling rates in different directions. However, they do not explain the relationship between the equation and hydrogeologic parameters or how the equation can be used to model solute plumes.
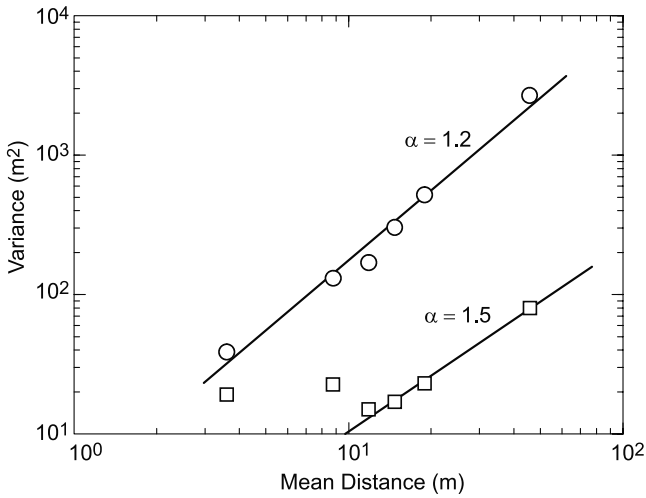
Figure 1. Measured longitudinal (circles) and lateral (squares) variance of the bromide plume versus mean travel distance from the MADE-1 test [*Adams and Gelhar*, 1992]. Lines indicate power laws of order 2/α. Transverse values are artificially high at early time due to the wide arrays of injection wells. From *Meerschaert et al.* [2001].

[5] Herein, we extend the theory of fractional ADEs in hydrogeology to multiple dimensions. By equating certain CTRW models of particle jump processes with the compound Poisson process, we interpret the meaning of the variables in the multiscaling spatially fractional ADE. Emphasis will be placed on the relationship between the mathematics and particle-jump models so that the rationale for using multiscaling fractional ADEs in contaminant transport modeling remains clear. We then develop a numerical procedure for computing the solutions to multiscaling ADEs.

2. Fractional Advection-Dispersion Equations

[6] Spatially fractional ADEs are used as models for stochastic processes with heavy-tailed independent increments or "jumps" [*Fogedby*, 1994; *Zaslavsky*, 1994a, 1994b; *Compte*, 1997; *Gorenflo and Mainardi*, 1997, 1998; *Saichev and Zaslavsky*, 1997; *Benson*, 1998; *Chaves*, 1998; *Metzler and Klafter*, 2000; *Baeumer and Meerschaert*, 2001]. The equations are subsets of the convolution-Fickian nonlocal ADEs described by *Cushman and Ginn* [1993, 2000]. As the scaling limits of sums of independent and identically distributed (iid) random variables, fractional ADEs are ergodic, nonlocal equations. This study will focus on spatially fractional processes for conservative solutes where the effects of spreading due to diffusion are negligible compared with those due to dispersion. The one-dimensional fractional ADE of form:

$$\frac{\partial C(x,t)}{\partial t} = -v\frac{\partial C(x,t)}{\partial x} + \frac{1}{2}(1+\beta)D\frac{\partial^{\alpha}}{\partial x^{\alpha}}C(x,t)$$
$$+ \frac{1}{2}(1-\beta)D\frac{\partial^{\alpha}}{\partial(-x)^{\alpha}}C(x,t), \qquad (1)$$

where $0 < \alpha \leq 2$ has been used to predict longitudinal plume growth at the Cape Cod and MADE test sites [*Benson et al.*, 2000, 2001]. Lévy's α-stable probability

density functions (PDF), with scale parameter α, spread parameter $\sigma = (D\,\Delta t)^{\frac{1}{2}}$, skewness parameter β, and shift parameter *v*, are the Green's function solutions to diffusion equations in which the second spatial derivative is replaced with a fractional derivative of order $0 < \alpha \leq 2$ The α-stable solutions have the Gaussian PDF as a subset when α = 2. This equation models a plume that grows at a rate proportional to t^{H} where $H = 1/\alpha$ is the scaling coefficient.

[7] A straightforward generalization of the fractional ADE and its solutions to multiple dimensions is possible when the order of the fractional derivative α is equal in all directions. This case, described by *Meerschaert et al.* [1999], has a constant order of differentiation in all directions:

$$\frac{\partial C(\vec{x},t)}{\partial t} = -\vec{v}\cdot\nabla C(\vec{x},t) + D\nabla^{\alpha}_{M}C(\vec{x},t), \qquad (2)$$

where ∇^{α}_{M} is a multivariate fractional derivative of order α. The multidimensional fractional ADE could be used to describe contaminant plume growth if the growth rates (scaling coefficients) in the longitudinal and transverse directions are equal.

[8] A multiscaling, spatially fractional ADE in which a scaling operator treats different scaling rates of dispersion in different directions was introduced by *Meerschaert et al.* [2001]:

$$\frac{\partial C(\vec{x},t)}{\partial t} = -\vec{v}\cdot\nabla C(\vec{x},t) + \nabla\cdot D_{F}\nabla C(\vec{x},t) + D\nabla^{H^{-1}}_{M}C(\vec{x},t), \quad (3)$$

where $\boldsymbol{H}^{-1}$ the inverse of the scaling matrix, provides the order and direction of the fractional derivatives. The structure of $\boldsymbol{H}^{-1}$ is described below. Without the last term on the right-hand side (RHS), equation (3) is the classical, multidimensional ADE. The first term treats linear advection, while the second term treats Fickian dispersion, if it exists, in any of the principal directions of plume growth. If dispersion is super-Fickian in all directions, then the Brownian motion modeled by the classical second-order dispersion tensor is overwhelmed. In this case, all components of the Fickian dispersion tensor, D_{F}, go to zero and the second term disappears. The third term on the RHS of (3), which treats heavy-tailed dispersion in the appropriate coordinates, is the subject of this study. The probabilistic interpretation of the fractional Laplacian $\nabla^{H^{-1}}_{M}$ with mixing measure M and matrix exponent $\boldsymbol{H}^{-1}$ is explored in detail. In this study, "multidimensional fractional ADE" will refer to the multivariate equation (2) with a single value of α governing fractional differentiation in all directions. "Multiscaling fractional ADE" will be used for the ADE with a matrix-order fractional operator (3). It should be emphasized that the term multiscaling refers to different scaling rates in different directions, not different scaling rates at different distances from the plume origin.

3. Stochastic Foundation of Multiscaling Dispersion

[9] For lack of microscopic or complete measuring tools, stochastic partial differential equations (PDE) are used to describe groundwater and aquifer contaminant movement at

measurable scales. Although the physical processes governing particle transport in aquifers are deterministic, the constitutive problem can be solved using probability theory as an analytical tool [*Bhattacharya and Gupta*, 1990]. The convention has been to view solute transport in aquifers as an ensemble of particles moving randomly through the porous medium, with each path line considered a vector sum of elementary particle displacements [*Bear*, 1972]. CTRWs, also-called renewal-reward processes, are generalizations of classical random walks in which the distance a particle has traveled is the sum of iid jumps governed by one probability distribution while the waiting times between the jumps are iid and governed by a second probability distribution [*Montroll and Weiss*, 1965; *Scher and Lax*, 1973]. The jump length and waiting time distributions can be independent of each other (uncoupled) or dependent and described by a single joint density (coupled). The waiting time can be thought of as the period between instantaneous jumps or as the time it takes for a jump to be completed. These stochastic processes have been applied to hydrogeology by *Berkowitz and Scher* [1995], *Berkowitz et al.* [2001], and *Benson* [1998]. CTRWs provide a useful model of aquifer solute transport; a particle can move through the aquifer with the groundwater or be motionless due to sorption or immobile zones. By taking the scaling limits of CTRWs, a variety of limit processes governed by PDEs are obtained. The limiting probability distribution governing total displacement of a single particle after a large number of displacements is then interpreted as the spatial distribution of a cloud of particles, or the concentration profile of an aquifer contaminant plume at a snapshot in time. The probability densities are the Green's function solutions to the PDEs.

[10] Spatially fractional and integer-order ADEs are the scaling limits of uncoupled CTRWs with finite mean waiting time distribution [*Compte*, 1996]. Finite mean waiting time CTRWs converge to the same limit processes as their corresponding classical random walks [*Barkai et al.*, 2000; *Whitt*, 2001; *Meerschaert et al.*, 2002]. As a result of a functional central limit theorem, random walks composed of normalized, iid finite-variance jumps converge in distribution to Brownian motion [*Billingsley*, 1968]. A Gaussian density is the Green's function solution to the ADE, which describes the location of a particle undergoing Brownian motion. Random walks with infinite variance jumps and a single tail parameter in all directions lead to α-stable Lévy motion, governed by multidimensional fractional ADEs (2). The limit of normalized sums of infinite variance random vectors with unique scaling parameters in each coordinate direction are operator stable distributions [*Meerschaert and Scheffler*, 2001]. Their densities are the Green's function solutions to the multiscaling fractional ADEs (3) that govern operator Lévy motions [*Sharpe*, 1969; *Meerschaert et al.*, 2001]. Operator stable distributions are the most general multivariate stable distributions, with independent tail parameters (α_i) in each direction [*Jurek and Mason*, 1993].

[11] The compound Poisson process is a subset of finite mean waiting time uncoupled CTRWs. In the following sections, we develop a probabilistic interpretation of multiscaling fractional dispersion based on the parameters of the compound Poisson process. The compound Poisson process

is used here for pedagogical purposes. All finite-mean waiting time CTRWs converge to the same limit processes as compound Poisson process.

3.1. Compound Poisson Process Particle Jump Model

[12] The CTRW with exponential waiting time distribution independent of the jump distribution corresponds with the compound Poisson process. To demonstrate, we first define the CTRW. Particle location at time t, $X(t)$, is the sum of random jumps, each with a random jump time:

$$X(t) = \sum_{n=1}^{N(t)} R_n \cdot \vec{\Theta}_n, \qquad (4)$$

where $N(t)$ is the number of random jumps by time t and R_n and $\vec{\Theta}_n$ are the random length and direction of the nth jump. The complete solution to the CTRW with independent jump sizes and durations is typically given by its Fourier-Laplace transform (denoted by change of variables $x \to k$ and $t \to s$, respectively) [*Scher and Lax*, 1973]:

$$\hat{\bar{P}}(k,s) = \frac{1 - \hat{\Psi}(s)}{s} \frac{1}{1 - \tilde{\phi}_o(k)\hat{\Psi}(s)}, \qquad (5)$$

where the probability of particle location $\hat{\bar{P}}(k,s)$ is a function of the jump size (and direction) distribution $\tilde{\phi}_o(k)$ and the waiting time distribution $\hat{\Psi}(s)$. Let the waiting time be exponentially distributed with Laplace transform $\hat{\Psi}(s) = \frac{\lambda}{\lambda + s}$. Then (5) simplifies to

$$\begin{aligned} \hat{\bar{P}}(k,s) &= \frac{1 - \frac{\lambda}{\lambda+s}}{s} \frac{1}{1 - \tilde{\phi}_o(k)\frac{\lambda}{\lambda+s}} \\ &= \frac{1}{s - \lambda(\tilde{\phi}_o(k) - 1)}. \end{aligned}$$

Inverse Laplace transform yields the Fourier transform of the compound Poisson process [*Feller*, 1968]:

$$\hat{P}(k,t) = \exp(\lambda t(\tilde{\phi}_o(k) - 1)), \qquad (6)$$

where λ and ϕ_o retain their meaning as jump rate parameter and jump size distribution, respectively. The compound Poisson process describes the location $X(t)$ of a particle as the sum of random jumps where the number of jumps $N(t)$ that occur by time t is a Poisson process. Since the waiting time distribution is exponential with mean $1/\lambda$ jumps have an average rate of occurrence λ Each jump has a random length and random direction so the jump distribution ϕ_o can be divided into a jump length distribution and a jump direction distribution. Jump direction is governed by a probability distribution known as the mixing measure $M(d\theta)$. For example, in the 1-D case, jumps are only permitted forwards or backwards and the discrete mixing measure is found directly in the terms of the 1-D fractional ADE (1) where

$$\begin{aligned} M(+1) &= \tfrac{1}{2}(1 + \beta) \\ M(-1) &= \tfrac{1}{2}(1 - \beta), \end{aligned} \qquad (7)$$

so $M(+1) + M(-1) = 1$ and $0 \leq \beta \leq 1$ defines the skewness of the process.

3.1.1. Multivariate (Multidimensional) Compound Poisson Process and Limits

[13] Infinite-variance jump lengths affect both the scaling and the tails of this CTRW in multiple dimensions. For example, if a single scaling coefficient $1/\alpha$ governs the growth rate in all directions, jumps may be written in the form $R^{1/\alpha}\vec{\Theta}$, where $R^{1/\alpha}$ represents the random jump length and $\vec{\Theta}$ is the jump direction random vector. Note that the jump magnitude is isotropic. This compound Poisson process describes particle location by

$$X(t) = \sum_{n=1}^{N(t)} R_n^{1/\alpha} \cdot \vec{\Theta}_n. \qquad (8)$$

Multidimensional random jumps $R^{1/\alpha}\vec{\Theta}$ are still described by the distribution $\phi_o(dr, d\theta)$. The heavy-tailed distribution of R is defined $P(R > r) \propto r^{-1}$ so that $P(R^{1/\alpha} > r) \propto r^{-\alpha}$. Also, the norm of the random jump direction vector $\| \vec{\Theta}_n \| = 1$, and R and $\vec{\Theta}$ are independent. The mixing measure $M(d\theta)$ governing jump direction where $P(\vec{\Theta} \in A) = M(A)$, can be continuous or discrete.

[14] The product of λ a positive real number that describes the average rate of motions, and ϕ_o a probability measure of jump size and direction, is a measure $\phi(dr, d\theta) = \lambda\phi_o(dr, d\theta)$ of total mass λ. This measure, known as the intensity measure or Lévy measure of the compound Poisson process [*Bertoin*, 1996 p.12], describes how often jumps of a given size and direction will occur. A measure assigns a value to a length or area and can be continuous or discrete. For example, a probability measure integrates the area under a probability density so that

$$\int_x^\infty \phi(dy) = \begin{cases} \int_x^\infty f(y)dy \text{ for a continuous probability measure} \\ \sum_x^\infty p(y) \text{ for a discrete probability measure.} \end{cases}$$
$$(9)$$

For any probability measure, $\int_{-\infty}^\infty \phi(dy) = 1$. A general measure follows the same rules, but the total mass of the measure need not be one. For the Lévy measure of the compound Poisson process described above, $\int_{-\infty}^\infty \phi(dy) = \lambda$.

[15] To make this particle jump process converge to a limit process, let the particle jump rate λ approach infinity, and at the same time, let the length of particle jumps approach zero. This subdivides motions into smaller and smaller units that occur with greater frequency, the usual process that transforms a random walk into a Brownian motion. Here, the sum of infinite variance particle jumps leads to Lévy motion [*Bertoin*, 1996; *Saichev and Zaslavsky*, 1997].

[16] Since particle jump length $R^{1/\alpha}$ is governed by a power law or Pareto probability distribution, its density looks like $a^\alpha \alpha r^{-\alpha-1}$ so that $\phi(dr, d\theta) = \lambda a^\alpha \alpha r^{-\alpha-1}$. The smallest jump permitted is of size a. Take the limit of this measure by rescaling in time ($\lambda \to \infty$) and space ($a \to 0$) The limit must be taken so that $\lambda a^\alpha \to D$, where D is a constant to avoid degenerate cases. The limiting form of the Lévy measure

$$\phi(dr, d\theta) = \alpha r^{-\alpha-1} dr D M(d\theta) \qquad (10)$$

describes the jump intensity of the Lévy motion and has directional and radial weights derived from a compound Poisson particle jump model. In approaching this limit, we also find that the dispersion coefficient D is dependent on the theoretical particle jump rate, particle jump length, and the order of the scaling exponent.

3.1.2. Multiscaling Compound Poisson Process and Limits

[17] When scaling rates vary with direction, R must be rescaled by $\boldsymbol{H}$, a matrix whose eigenvalues are the scaling coefficients $1/\alpha_i$ of the growth process. Then the multiscaling compound Poisson process is defined

$$X(t) = \sum_{n=1}^{N(t)} R_n^H \cdot \vec{\Theta}_n. \qquad (11)$$

As in the standard multidimensional case, $P(R > r) \propto r^{-1}$ and $P(\vec{\Theta} \in A) = M(A)$. The matrix $R^{\boldsymbol{H}}$ is now anisotropic with different jump sizes in different directions. Jump length probabilities on the ith eigenvector fall off as $r^{-\alpha_i}$ while jump length probabilities on trajectories off the eigenvectors fall off like powers of a mixture of the scaling coefficients.

[18] Multiscaling compound Poisson processes converge to operator Lévy motion [*Meerschaert et al.*, 2002]. The Lévy measure $\phi(dr, d\theta)$ in (10) is valid for multidimensional ADEs with a single fractional derivative describing scaling in every direction, governing multivariate Lévy motion. The varied effect of a velocity change in one direction on multiscaling dispersion in all directions is controlled by the scaling matrix $\boldsymbol{H}$ When the Lévy measure is expressed in a coordinate system adapted to the matrix $\boldsymbol{H}$ (described below), the jump probabilities in all directions are equal.

3.2. Relation of Model Variables to Hydraulic Properties

[19] The parameters in the compound Poisson particle jump model for solute dispersion can be related to hydraulic properties. The mixing measure $M(d\theta)$ describing the jump direction density, is dependent on the hydraulic conductivity field and the direction of the hydraulic gradient. Preferential pathways will be represented in the mixing measure by larger jump probabilities in their respective directions. If the hydraulic conductivity in two directions is equal, the direction closer to the gradient will be weighted more heavily in the mixing measure. While an aquifer conductivity field remains constant, the magnitude of the velocity field may fluctuate in time. As in the classical ADE, the dispersion coefficient measures the difference in particle velocities. The change in particle jump size due to velocity fluctuations is represented by a change in the dispersion coefficient, a linear function of the compound Poisson rate parameter λ. If the average linear velocity is doubled, the particle jump rate will be doubled, and in turn, the dispersion coefficient will be doubled. This is in keeping with the traditional notion that the dispersion coefficient is linear with the hydraulic gradient or velocity field [*Bear*, 1972]. In 1-D, $\boldsymbol{H}^{-1} = 1/H = \alpha$ has been related to the degree of heterogeneity in an aquifer [*Schumer et al.*, 2001]. Greater heterogeneity implies greater deviation from the mean particle velocity, allowing for an increased rate of scaling or super-Fickian plume growth. When $\boldsymbol{H}^{-1}$ is a matrix, smaller coefficients still correspond with a greater degree of heterogeneity. Since

dispersion is proportional to velocity and larger average velocities are found in the longitudinal direction of aquifers, the rate of scaling will be larger in the longitudinal direction than the transverse direction of solute plumes and the coefficients will be smallest in the longitudinal direction.

4. Multiscaling Fractional ADEs

[20] The multiscaling fractional ADE treats Fickian plume growth in any direction in the same manner as the classical ADE. It can also model super-Fickian plume growth with unique scaling rates in any direction. The multivariate Gaussian is notable among the α-stable distributions because it has no skewness and its spread is described by a covariance matrix rather than a mixing measure. Random walks with finite-variance particle jumps converge to Brownian motion with Gaussian distributions while infinite-variance random walks converge to Lévy motion with non-Gaussian α-stable distributions. Brownian motion models imply scaling by second-order derivatives (since $H^{-1} = (1/2)^{-1} = 2$) while non-Gaussian stables imply fractional derivatives. The two classes of stable distribution are sufficiently different that they can not be treated by the same operator. As a result, a Gaussian term and a heavy-tailed term appear in the multiscaling fractional ADE (3). If particle dispersion in a given aquifer is due to heavy-tailed jumps in at least one direction and Gaussian dispersion in at least one other, then the multiscaling fractional ADE treats them independently [*Meerschaert et al.*, 2001].

4.1. Multiscaling Fractional Derivatives

[21] The properties of fractional derivatives are described by *Oldham and Spanier* [1974], *Samko et al.* [1993], and *Miller and Ross*, [1993]. The fractional operator ∇_M^α of multidimensional ADEs (2), is a linear combination of directional derivatives, all of order α with mixing measure M providing the relative weights in all directions [*Meerschaert et al.*, 1999]. In multiscaling fractional ADEs, anomalous dispersion is modeled by the multiscaling fractional derivative $\nabla_M^{H^{-1}}$. This nonlocal fractional operator is defined by [*Meerschaert et al.*, 2001]:

$$\nabla_M^{H^{-1}} C(x) = \int\limits_0^\infty [C(x-y) - C(x) + y \cdot \nabla C(x)] \phi(dy), \quad (12)$$

with Fourier transform

$$F\left[\nabla_M^{H^{-1}} C(\vec{x})\right] = \left(\int \left(e^{-i\vec{k}\cdot\vec{x}} - 1 + i\vec{k}\cdot\vec{x}\right)\phi(d\vec{x})\right)\hat{C}\left(\vec{k}\right). \quad (13)$$

The Fourier transform of the fractional derivative (13) is equivalent to the Fourier transform of the mean-centered compound Poisson distribution (Appendix A) so the Lévy measure $\phi(d\vec{x})$ can be equated with the limiting form of the compound Poisson Lévy measure, a function of H^{-1} and M. Particles undergoing fractional dispersion from any starting point will move in a random direction governed by the mixing measure M of the fractional derivative. Associated with each direction is a jump length distribution.

[22] Computations in Lemma 7.3.8 of *Meerschaert and Scheffler* [2001] show that, in one dimension,

$$\int (e^{-ikx} - 1 + ikx)\phi(dx)\hat{C}(k) = (ik)^\alpha \hat{C}(k)$$

This is a simple convolution of the concentration with a power law (in the sense of distributions, see *Rudin* [1991]): $\frac{d^\alpha C(x)}{dx^\alpha} = \frac{1}{\Gamma(-\alpha)} \int r^{-\alpha-1} C(x-r) dr$. The fractional derivative models a redistribution of the concentration at all points according to a power law of the distance r. The multi-dimensional generalization (13) is a redistribution of solute according to various power laws in each direction. Because of the link with the particle jump model, this implies that the jump length distribution in each direction decays as a unique power law prescribed by H^{-1} After a particle has made many of these power law jumps, the density $C(x, t)$ describing its random location will grow in several dimensions according to the scaling matrix H. Detailed discussions of the form of the scaling matrix H and the mixing measure M follow.

4.1.1. Scaling Matrix H

[23] The scaling matrix H describes the scale invariance of the PDF used to represent the contaminant plume. The solutions $C(x, t)$ to 1-D fractional ADEs grow as $C(x, Kt) = K^{-1/\alpha}C(K^{-1/\alpha}x, t)$, where K is a constant. Similarly, the density of particle location governed by a multiscaling fractional ADE scales as $C(\vec{x}, Kt) = |K^{-H}|C(K^{-H}\vec{x}, t)$, where $|\cdot|$ is the determinant. If the primary directions of growth are perpendicular, as might be assumed for flow in granular porous media, then the scaling terms in each of the principal directions $1/\alpha_j$ are the eigenvalues of the matrix H and it is of the form $H_o = \begin{bmatrix} 1/\alpha_x & 0 & 0 \\ 0 & 1/\alpha_y & 0 \\ 0 & 0 & 1/\alpha_z \end{bmatrix}$, where H_o will be used for a diagonal eigenvalue matrix. In this case, plume growth in direction j scales by a power of $1/\alpha_j$. Since the exponents $1/\alpha_j$ reflect the self-similarity of the random process, they are sometimes called the Hurst indices.

[24] The multiscaling fractional ADE can describe plume growth with nonorthogonal principal growth directions. This represents a departure from previous methods for describing plume scaling and points toward the description of plume growth in fracture networks. The form of the matrix H describing nonorthogonal flow directions can be calculated by a change of basis, or similarity transformation. The matrix H will have the same eigenvalues as its eigenvalue matrix H_o, but eigenvectors along the fractures, rather than the x, y, and z axes. Then the scaling matrix H in Cartesian coordinates will be diagonalized by the equation

$$H_o = S^{-1}HS, \quad (14)$$

where H_o and S are, respectively, the eigenvalues and eigenvector matrices for H [*Strang*, 1988]. By their physical interpretation, we assume the eigenvalues and eigenvectors of H in groundwater transport applications will always exist, guaranteeing that the matrix is diagonalizable. Since the eigenvectors of H, which correspond to the fracture directions, are known, H can be calculated by $H = SH_oS^{-1}$. For example, working in two dimensions, if fractures occur at $0°$ and $30°$ the eigenvectors will be $\begin{bmatrix} 1 \\ 0 \end{bmatrix}$ and $\begin{bmatrix} \frac{\sqrt{3}}{2} \\ 1/2 \end{bmatrix}$. Then, the scaling matrix will be

$$H = \begin{bmatrix} 1 & \frac{\sqrt{3}}{2} \\ 0 & \frac{1}{2} \end{bmatrix} \begin{bmatrix} \frac{1}{\alpha_1} & 0 \\ 0 & \frac{1}{\alpha_2} \end{bmatrix} \begin{bmatrix} 1 & -\sqrt{3} \\ 0 & 2 \end{bmatrix} = \begin{bmatrix} \frac{1}{\alpha_1} & \frac{\sqrt{3}}{\alpha_2} - \frac{\sqrt{3}}{\alpha_1} \\ 0 & \frac{1}{\alpha_2} \end{bmatrix}.$$

Table 1. Definitions of Stochastic Measures Used in Particle Jump Models

Parameter	Symbol	Meaning
Mixing measure	$M(d\theta)$	specifies the probability of a particle jumping through segment $d\theta$ of the unit circle
Spectral measure	$\Lambda(d\theta) = DM(d\theta)$	specifies the probability and relative magnitude of particle jumps
Lévy measure	$\phi(dr, d\theta)$ $= \alpha r^{-\alpha-1} dr\, \Lambda(d\theta)$ $= \alpha r^{-\alpha-1} dr DM(d\theta)$ (multidimensional form)	specifies the probability of jumps of a given size in each direction θ

If fractures occur at $\pm 30°$ then

$$H = \begin{bmatrix} \frac{\sqrt{3}}{2} & \frac{\sqrt{3}}{2} \\ \frac{1}{2} & \frac{-1}{2} \end{bmatrix} \begin{bmatrix} \frac{1}{\alpha_1} & 0 \\ 0 & \frac{1}{\alpha_2} \end{bmatrix} \begin{bmatrix} \frac{\sqrt{3}}{3} & 1 \\ \frac{\sqrt{3}}{3} & -1 \end{bmatrix} = \begin{bmatrix} \frac{1}{2\alpha_1} + \frac{1}{2\alpha_2} & \frac{\sqrt{3}}{2\alpha_1} - \frac{\sqrt{3}}{2\alpha_2} \\ \frac{\sqrt{3}}{6\alpha_1} - \frac{\sqrt{3}}{6\alpha_2} & \frac{1}{2\alpha_1} + \frac{1}{2\alpha_2} \end{bmatrix}.$$

The inverse of the scaling matrix H^{-1} is the matrix order of differentiation in the multiscaling fractional ADE. Each eigenvalue of H^{-1} is the order of the fractional derivatives in a principal direction of growth (the eigenvectors). When the principal directions of growth are along the standard Cartesian axes, the order of the fractional derivatives are the reciprocal to the scaling coefficients.

4.1.2. Mixing Measure $M(d\theta)$ and Spectral Measure $\Lambda(d\theta)$

[25] While H dictates the plume scaling characteristics, the mixing measure $M(d\theta)$ defines the shape and skewness of the plume. The definition of $M(d\theta)$ comes from the compound Poisson process, where it represents the proportion of jumps in each angular interval $d\theta$. The dispersion coefficient D specifies the frequency of these jumps. Studies on heavy-tailed random vector parameter estimation refer to the spectral measure, the product of the mixing measure and the dispersion coefficient, as a single variable [*Nolan*, 1998] (see Table 1.) We adopt the same notation because analysis of plume characteristics will likely yield an estimate of the spectral measure, rather than individual values of D and $M(d\theta)$.

[26] A spectral measure $\Lambda(d\theta)$ on the unit sphere assigns weights corresponding with probability of jumps in each direction and defines the properties that reduce to skewness (β) and spread (σ) in one dimension. The mixing measure is a probability measure with total mass $\int_\theta M(d\theta) = 1$. The spectral measure has mass $\int_\theta \Lambda(d\theta) = D$. The spectral measure can be continuous or discrete. When the spectral measure is uniform, the probability of particle jumps is equal in all directions and the multivariate stable density is symmetric (Figure 2a). When the spectral measure is discrete and concentrated on the intersection of the axes with the unit sphere (i.e., $\{1, 0\}$, $\{0, 1\}$, $\{-1, 0\}$, $\{0, -1\}$), then particle jumps are only possible to the north, south, east and west (Figure 2b). In this special case, the particle jumps in each direction, representing longitudinal and transverse dispersion, are independent [*Samorodnitsky and Taqqu*, 1994; *Nolan*, 1998]. This highlights the notion that in assigning particle jump weights in every direction around a unit circle or sphere, the spectral measure defines the dependence between jumps in each of the principal directions.

[27] Since the spectral measure describes the most probable directions of transport, we expect the weight of the spectral measure of a porous medium to be greatest in the principal flow direction, with decreasing weight toward the transverse directions. A conservative contaminant plume will have a spectral measure indicating a higher probability of particle velocities above the mean velocity than below (Figure 2c). Spikes in the spectral measure may occur in a preferential flow path direction where there is an increased probability of particle movement.

[28] Operator Lévy motions in d-dimensions may have up to d unique heavy-tailed components. In the limit, any others are overwhelmed by the d heaviest motions. To illustrate, consider jumps allowed in 3 directions in 2-D, with $\alpha_a = 1.1$, $\alpha_b = 1.3$, and $\alpha_c = 1.5$. In the limit, the large jumps in the a and b directions stand out and the effects of the heavy-tailed process in the c direction will not be discernible. Jumps will still occur in the c direction in the mixing measure but the limiting operator stable will only have 2 principal scaling directions. In this case, H^{-1} will have eigenvectors equal to directions a and b and eigenvalues α_a and α_b.

### 4.2. Solutions to Multiscaling Fractional ADEs

[29] The Green's function solution to multiscaling fractional ADEs can be calculated using Fourier transforms:

$$\frac{\partial \hat{C}(\vec{k}, t)}{\partial t} = \left[\left(-i\vec{v} \cdot \vec{k} \right) + \left(i\vec{k} \right) \cdot D_F \left(i\vec{k} \right) \right. \\ \left. + \int \left(e^{-i\vec{k}\cdot\vec{x}} - 1 + i\vec{k} \cdot \vec{x} \right) \phi\left(d\vec{k} \right) \right] \hat{C}(\vec{k}, t)$$

Solving for $\hat{C}(\vec{k}, t)$ with an instantaneous release at the origin $C(\vec{0}, 0) = 1$ yields

$$\hat{C}(\vec{k}, t) = \exp\left[t\left(-i\vec{v} \cdot \vec{k} - \vec{k} \cdot Q\vec{k} \right. \right. \\ \left. \left. + \int \left(e^{-i\vec{k}\cdot\vec{x}} - 1 + i\vec{k} \cdot \vec{x} \right) \phi(d\vec{x}) \right) \right], \qquad (15)$$

where Q is a covariance matrix. This Fourier transform, known as the Lévy representation, simplifies to common parameterization of the 1-D and multivariate α-stable characteristic functions (as in the work of *Samorodnitsky and Taqqu* [1994]) when the proper power law Lévy measure is applied [*Meerschaert and Scheffler*, 2001, chap. 7]. There is no simplified form for operator stable
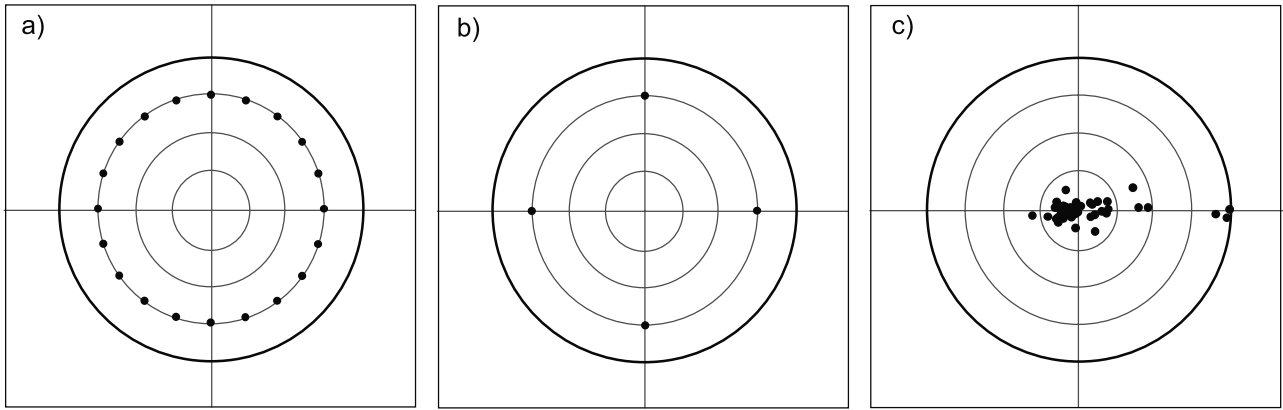
Figure 2. (a) Discrete, uniform spectral measure. (b) Measure concentrated on coordinate axes representing independent jump probabilities. (c) Possible spectral measure for a particle jump model representing plume growth.

densities, so the Lévy representation (15) is used to represent them.

5. Computation and Application of Operator Stable Densities

[30] A coordinate system adapted to the scaling matrix is introduced above. The Jurek coordinate system allows for the independent representation of the scale parameters and spectral measure in the Lévy measure $\phi(d\vec{x})$. Since these are the variables that can be related to aquifer transport properties, this coordinate system must be used to express the Fourier transform of operator stable densities. A description of the Jurek coordinate system is followed by the procedure for generating solutions to multiscaling fractional ADEs and a discussion of hydrogeologic applications.

5.1. Jurek Coordinate System

[31] The Jurek coordinate system is an anisotropic polar coordinate system. The jump probability level sets of the spectral measure are ellipses (Figure 3). If the order of differentiation α is equal to 1.1 in both the x and y directions, the probability of a particle jump length of 1.5 units is equally probable in all directions, so the $r_j = 1.5$ coordinate line is circular (Figure 3a). If α_y is increased to 1.6 (less heavy-tailed,) it is less likely that

particles will jump as far in the y direction and longer jumps are given more weight in that direction (Figure 3b). This feature is more apparent as α_y is increased to 1.9 (Figure 3c).

[32] In the Jurek coordinate system, r_j, the analogue to the polar r is curved so that it is orthogonal to (independent of) the ellipses. As in standard polar coordinates, θ denotes the angle at which r_j crosses the unit circle (the 1 coordinate line in Figures 3a, 3b, and 3c). However, this angle only corresponds with the angle between r_j and the x axis at the origin when the scaling parameters are equal in all directions and the Jurek coordinate system reduces to a rescaled polar coordinate system where $r_j = r^{1/\alpha}$. When all $\alpha_i = 1$ the Jurek coordinate system is equivalent to the standard polar coordinate system.

[33] Transformation from Cartesian to Jurek coordinates requires the conversion $\vec{x} = r_j^H \vec{\theta}$. For example, if H is symmetric then $x_1 = r_j^{1/\alpha_1} \cos \theta$ and $x_2 = r_j^{1/\alpha_2} \sin \theta$. *Jurek and Mason* [1993] provide the form of the Lévy measure in Jurek coordinates:
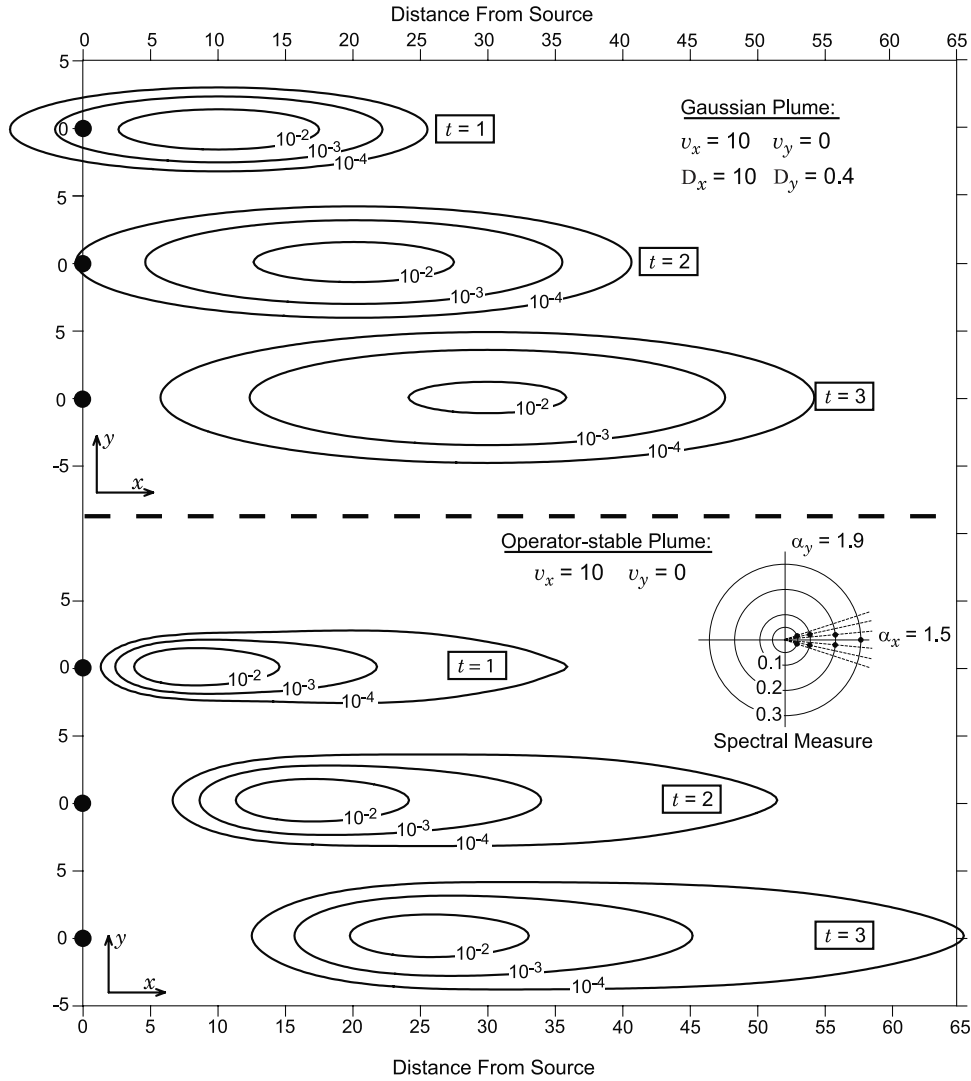
$$\phi(dx) = \frac{dr_J}{r_J^2} \Lambda(d\theta). \tag{16}$$

This conversion can be read $\int f(\vec{x})d\vec{x} \rightarrow \int \int g(\vec{\theta})\frac{1}{r_j^2}dr_j d\theta$, resembling a typical Cartesian to polar coordinates conver-
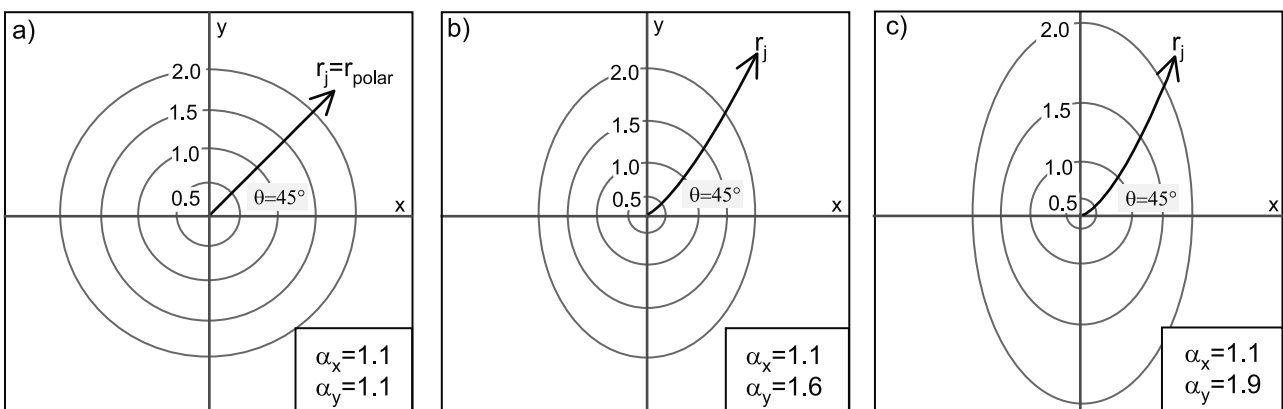
Figure 3. Comparison of level sets in the Jurek coordinate system for various combinations of α_x and α_y.

Figure 4. Growth of Gaussian versus operator stable plumes with time. The Gaussian plume follows equation (2) with $\alpha = 2$. Each plume has a mass of unity and mean velocity of 10 in the positive x direction. Relative to the x axis, the spectral measure has points at $0°$, $\pm6°$, $\pm12°$, and $\pm18°$, with increasing intensity in the direction of mean travel. The initial condition is a Dirac delta function denoted by the heavy filled circles.

sion where $1/r_j$ is the scaling required for the change of variables in (16).

[34] In the Jurek coordinate system, the solution to multiscaling ADEs is the Lévy representation for an operator stable density [*Meerschaert and Scheffler*, 2001]:

$$\hat{C}\left(\vec{k},t\right) = \exp\left(i\vec{\mu}_2 \cdot \vec{k} \int_{\|\theta\|=1} \int_{r_J=0}^{\infty} \left(e^{i\vec{k}\cdot r_J^H \theta} - 1 - i\vec{k}\cdot r_J^H \theta \right) \right.$$

$$\left. \cdot \frac{dr_J}{r_J^2}\Lambda(d\theta) \right)t. \tag{17}$$

5.2. Calculation of Operator Stable Densities

[35] In most cases, there is no closed form analytical expression for operator stable densities. This computation was performed by transforming the discrete counterpart of (17) to real space using a Fast Fourier Transform (FFT). The

singularities and oscillations in the integrand of (17) were treated individually to ensure convergence and accuracy. A MathCAD worksheet (obtainable from the authors) that calculates two-dimensional operator stable densities given a shift vector and spectral measure was developed and used to generate the figures described in the following section. This worksheet was verified for the multidimensional case (α equal in all directions) using the code described by *Nolan* [1998].

5.3. Model Application in Hydrogeology

[36] The flexible scaling rates and heavy leading edges of non-Gaussian operator stable densities capture some of the anomalous behavior of real contaminant plume growth unattainable by a Gaussian density (Figure 4). The asymmetry of a spectral measure leads to skewness and slowly moving peak values of operator stable densities (Figure 4).

[37] Multiscaling fractional ADEs may also be useful in modeling solute transport in noncontinuum, or discrete,
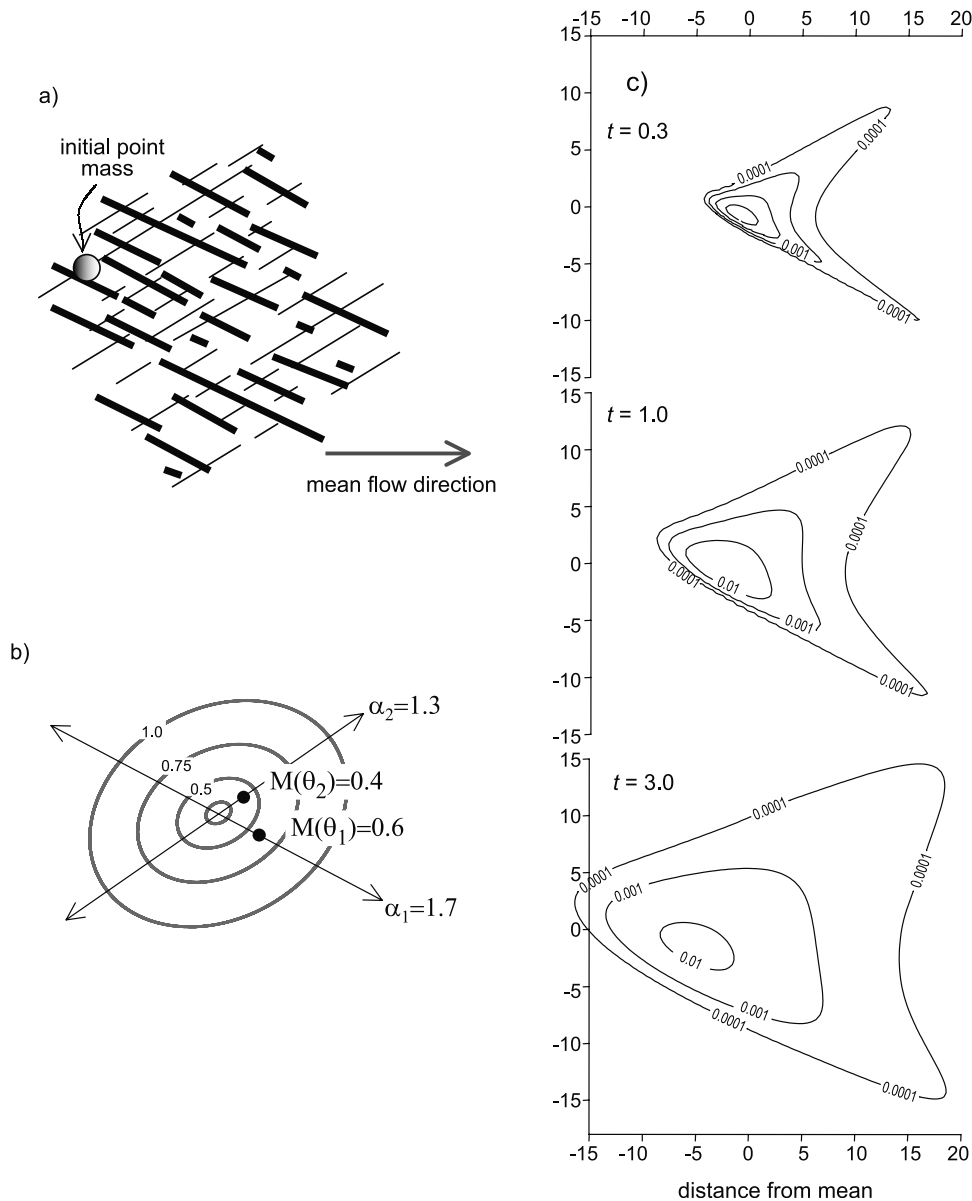
Figure 5. A conceptual model of plume growth in a fractured aquifer: (a) noncontinuum conceptual model, (b) operator stable parameters, and (c) operator stable densities with time. Note the greater mass in the θ_1 direction at early time due to the spectral measure, but the greater growth rate in the θ_2 direction due to smaller α_1.

fracture networks (Figure 5a). Use of a single analytical equation to describe multidimensional transport in fractured aquifers would be a novel approach. Solute transport in simple fracture networks is typically modeled using discrete network models, equivalent continuum models, or a combination of the two [*National Research Council*, 1996]. Various deterministic and probabilistic techniques can be used to create these heterogeneous flow domains before numerical solutions to the classical ADE or particle tracking methods are applied [*Clemo and Smith*, 1997]. The same probabilistic techniques may be used to estimate the parameters of an operator stable model of fractured-aquifer plume growth. The percentage of fractures in classes of orientations, along with the mean apertures and degree of connectivity, gives the spectral measure (Figure 5b). The scaling rate along a preferred fracture direction (α_j) may be more difficult to estimate a priori, but will depend on the variability of fracture length and aperture in a given orientation. With estimates of these two parameters, the corresponding operator stable densities yields the probabilistic concentration profiles predicted by the multiscaling fractional ADE with time (Figure 5c). Notable is the prediction of the greatest plume growth and earliest breakthrough along preferred fracture directions instead of directly downgradient of the source. Furthermore, at early time, the longer finger is observed in the direction of the wider fractures ($M(\theta_1) = 0.6$) but is surpassed at later times by the finger in the direction of the greater scaling rate ($\alpha_2 = 1.3$) The same concentration level sets are used in the three operator stable densities shown in Figure 5c, making it appear that the snapshots are becoming less heavy-tailed with time along the fracture directions. However, if level

sets representing smaller concentrations were used in subsequent snapshots, it would be apparent that the fingers remain ahead of the majority of the plume for all time.

6. Summary

[38] CTRW models of particle transport converge to stochastic limit processes governed by PDEs. Compound Poisson processes with arbitrary jump distribution and finite mean waiting time distribution lead to operator Lévy motion, governed by multiscaling fractional ADEs. These equations describe linear advection and Fickian or super-Fickian dispersion. The super-Fickian dispersive term $D \nabla_M^{H^{-1}} C(\vec{x}, t)$ of multiscaling fractional ADEs has a fractional derivative of matrix order. The scaling matrix H describes the scaling of the contaminant plume growth, and the inverse of this matrix contains the order (eigenvalues) and directions (eigenvectors) of fractional differentiation. The eigenvectors of the growth process can be orthogonal (as in granular aquifers) or nonorthogonal (as in fracture flow). In d dimensions as many as d independent scaling rates remain in the limit. The mixing measure $M(d\theta)$ specifies the proportion of particle jumps in every direction while the dispersion coefficient D describes the overall jump intensity given the scaling coefficients from the scaling matrix H. The operator stable densities that solve multiscaling fractional ADEs can be computed via Fourier transform using a modified polar coordinate system we call the Jurek coordinate system. These solutions capture essential features of real plumes, including different growth rates in different directions and skewed and/or fingered plumes.

Appendix A: Equivalence of Compound Poisson and Multiscaling Fractional Derivative Transforms

[39] Demonstration that the Fourier transforms of the multiscaling fractional derivative and mean-centered compound Poisson process are equivalent requires the definition of b the average particle jump length (assuming one exists). Equation (6) gave the Fourier transform of the compound Poisson distribution

$$E\left(e^{-ikX}\right)_{\text{compound Poisson}} = \exp\left(\lambda\left(\tilde{\phi}_o(k) - 1\right)\right).$$

Then, using the relations $\hat{\phi}_o(k) = \int e^{-ikx}\phi_o(dx)$, $\int \phi_o(dx) = 1$, and $\int x\phi_o(dx) = E[x] = b$, the Fourier transform for a centered compound Poisson $Y = X - b\lambda$ is

$$\begin{aligned} E\left(e^{-ikY}\right) &= \exp\left[\lambda\left(\hat{\phi}_o(k) - 1\right) - (-ik)\lambda b\right] \\ &= \exp\left[\left(\lambda\left(\hat{\phi}_o(k) - 1\right) + (ik)\lambda b\right)\right] \\ &= \exp\left[\lambda\left(\int e^{-ikx}\phi_o(dx) - \int \phi_o(dx)\right) + ik\lambda \int x\phi_o(dx)\right] \\ &= \exp\left[\int\left(e^{-ikx} - 1 + ikx\right)\lambda\phi_o(dx)\right]. \end{aligned}$$

Expressing the Fourier transform for a centered compound Poisson process in terms of the intensity measure we have

$$E\left(e^{-ikY}\right) = \exp\left[\int\left(e^{-ikx} - 1 + ikx\right)\phi(dx)\right],$$

which was given as the Fourier transform of the multiscaling fractional derivative in (13).

Notation

C solute concentration, ML^{-3}.
X Pareto shift parameter.
D_F Fickian dispersion tensor, $L^2 t^{-1}$.
D generalized dispersion coefficient, $L^\alpha t^{-1}$.
$\vec{k}$ wave vector, L^{-1}.
H scaling matrix.
M mixing measure.
Q covariance matrix
R jump length variable, L.
v average solute velocity, Lt^{-1}.
α order of fractional differentiation/α-stable tail parameter.
β α-stable skewness parameter.
σ α-stable spread parameter.
Λ spectral measure.
θ angle around the unit circle, radians.
$\vec{\Theta}$ unit vector.
ϕ Lévy measure.
ϕ_o jump length measure.
λ Poisson rate parameter, $\#t^{-1}$.
Ψ waiting time distribution.

References

Adams, E. E., and L. W. Gelhar, Field study of dispersion in a heterogeneous aquifer, 2, Spatial moments analysis, *Water Resour. Res.*, *28*(12), 3293–3397, 1992.

Baeumer, B., and M. M. Meerschaert, Stochastic solutions for fractional Cauchy problems, *Fractional Calculus Appl. Anal.*, *4*(4), 481–500, 2001.

Barkai, E. R. M., and J. Klafter, From continuous time random walks to the fractional Fokker-Planck equation, *Phys. Rev. E*, *61*, 132–138, 2000.

Bear, J., *Dynamics of Fluids in Porous Media*, Elsevier Sci., New York, 1972.

Benson, D. A., The fractional advection-dispersion equation: Development and application, Ph.D. thesis, Univ. of Nev., Reno, 1998.

Benson, D. A., S. W. Wheatcraft, and M. M. Meerschaert, Application of a fractional advection-dispersion equation, *Water Resour. Res.*, *36*(6), 1403–1412, 2000.

Benson, D. A., R. Schumer, M. M. Meerschaert, and S. W. Wheatcraft, Fractional dispersion, Lévy motion, and the MADE tracer tests, *Transp. Porous Media*, *42*, 211–240, 2001.

Berkowitz, B., and H. Scher, On characterization of anomalous dispersion in porous and fractured media, *Water Resour. Res.*, *31*(6), 1461–1466, 1995.

Berkowitz, B., G. Kosakowski, G. Margolin, and H. Scher, Application of continuous time random walk theory to tracer test measurements in fractured and heterogeneous porous media, *Ground Water*, *39*(4), 593–604, 2001.

Bertoin, J., *Lévy Processes*, Cambridge Univ. Press, New York, 1996.

Bhattacharya, R., and V. K. Gupta, Application of central limit theorems to solute dispersion in saturated porous media: from kinetic to field scales, in *Dynamics of Fluids in Hierarchical Porous Media*, edited by J. H. Cushman, pp. 61–95, Academic, San Diego, Calif., 1990.

Billingsley, P., *Convergence of Probability Measures*, John Wiley, New York, 1968.

Chaves, A. S., A fractional diffusion equation to describe Lévy flights, *Phys. Lett. A*, *239*, 13–16, 1998.

Clemo, T., and L. Smith, A hierarchical model for solute transport in fractured media, *Water Resour. Res.*, *33*(8), 1763–1783, 1997.

Compte, A., Stochastic foundations of fractional dynamics, *Phys. Rev. E*, *53*(4), 4191–4193, 1996.

Compte, A., Continuous time random walks on moving fluids, *Phys. Rev. E*, *55*(6), 6821–6831, 1997.

Cushman, J. H., and T. R. Ginn, Nonlocal dispersion in media with continuously evolving scales of heterogeneity, *Transp. Porous Media*, *13*, 123–138, 1993.

Cushman, J. H., and T. R. Ginn, The fractional ADE is a classical mass balance with convolution–Fickian flux, *Water Resour. Res.*, *36*(12), 3763–3766, 2000.

de Josselin de Jong, G., Longitudinal and transverse diffusion in granular deposits, *Eos Trans. AGU*, *39*(1), 67–74, 1958.

Feller, W., *An Introduction to Probability Theory and Its Applications*, vol. I, John Wiley, New York, 1968.

Fogedby, H. C., Lévy flights in random environments, *Phys. Rev. Lett.*, *73*(9), 2517–2520, 1994.

Gorenflo, R., and F. Mainardi, Fractional calculus: Integral and differential equations of fractional order, in *Fractals and Fractional Calculus in Continuum Mechanics*, edited by A. Carpinteri and F. Mainardi, pp. 223–276, Springer-Verlag, New York, 1997.

Gorenflo, R., and F. Mainardi, Random walk models for space-fractional diffusion processes, *Fractional Calculus Appl. Anal.*, *1*, 167–191, 1998.

Jurek, Z. J., J. D. Mason, *Operator-Limit Distributions in Probability Theory*, John Wiley, New York, 1993.

Mainardi, F., Y. Luchko, and G. Pagnini, The fundamental solution of the space-time fractional diffusion equation, *Fractional Calculus Appl. Anal.*, *4*, 153–192, 2001.

Meerschaert, M. M., H. P. Scheffler, *Limit Theorems for Sums of Independent Random Vectors: Heavy Tails in Theory and Practice*, John Wiley, New York, 2001.

Meerschaert, M. M., D. A. Benson, and B. Baeumer, Multidimensional advection and fractional dispersion, *Phys. Rev. E*, *59*, 5026–5028, 1999.

Meerschaert, M. M., D. A. Benson, and B. Baeumer, Operator Lévy motion and multiscaling anomalous diffusion, *Phys. Rev. E*, *63*, 021112–021117, 2001.

Meerschaert, M. M., D. A. Benson, H.-P. Scheffler, and B. Baeumer, Stochastic solution of space-time fractional diffusion equations, *Phys. Rev. E.*, *65*, 041113–041116, 2002.

Metzler, R., and J. Klafter, The random walk's guide to anomalous diffusion: A fractional dynamics approach, *Phys. Rep.*, *339*, 1–77, 2000.

Miller, K. S., B. Ross, *An Introduction to Fractional Calculus and Fractional Differential Equations*, John Wiley, New York, 1993.

Montroll, E. W., and G. H. Weiss, Random walks on lattices, II, *J. Math Phys.*, *6*(2), 167–181, 1965.

National Research Council, *Rock Fractures and Fluid Flow: Contemporary Understanding and Applications*, Natl. Acad. Press, Washington, D. C., 1996.

Nolan, J. P., Multivariate stable distributions: Approximation, estimation, simulation and identification, in *A Practical Guide to Heavy Tails: Statistical Techniques and Applications*, edited by R. J. Adler, R. Feldman, and M. Taqqu, Birkhäuser Boston, Cambridge, Mass., 1998.

Oldham, K. B., and J. Spanier, *The Fractional Calculus: Theory and Applications of Differentiation and Integration to Arbitrary Order*, Academic, San Diego, Calif., 1974.

Pachepsky, Y., D. A. Benson, and W. Rawls, Simulating scale-dependent solute transport in soils with the fractional advective-dispersive equation, *Soil Sci. Soc. Am. J.*, *64*(6), 1234–1243, 2000.

Rudin, W., *Functional Analysis*, 2nd ed., McGraw-Hill, New York, 1991.

Saichev, A. I., and G. M. Zaslavsky, Fractional kinetic equations: Solutions and applications, *Chaos*, *7*(4), 753–764, 1997.

Samko, S. G., A. A. Kilbas, and O. I. Marichev, *Fractional Integrals and Derivatives: Theory and Applications*, Gordon and Breach, Newark, N. J., 1993.

Samorodnitsky, G., and M. S. Taqqu, *Stable Non-Gaussian Random Processes: Stochastic Models with Infinite Variance*, Chapman and Hall, New York, 1994.

Scher, H., and M. Lax, Stochastic transport in a disordered solid, II, Impurity conduction, *Phys. Rev. B*, *7*(10), 4502–4512, 1973.

Schumer, R., D. A. Benson, M. M. Meerschaert, and S. W. Wheatcraft, Eulerian derivation for the fractional advection-dispersion equation, *J. Contam. Hydrol.*, *48*, 69–88, 2001.

Sharpe, M., Operator-stable probability distributions on vector groups, *Trans. Am. Math. Soc.*, *136*(51), 51–65, 1969.

Strang, G., *Linear Algebra and its Applications*, 3rd ed., Harcourt Brace Jovanovich, Fort Worth, Ind., 1988.

Whitt, W., *Stochastic-Process Limits*, Springer-Verlag, New York, 2001.

Zaslavsky, G. M., Renormalization group theory of anomalous transport in systems with Hamiltonian chaos, *Chaos*, *4*(1), 25–33, 1994a.

Zaslavsky, G. M., Fractional kinetic equation for Hamiltonian chaos, *Physica D*, *76*, 110–122, 1994b.

B. Baeumer, Department of Mathematics and Statistics, University of Otago, Dunedin, New Zealand.

D. A. Benson and R. Schumer, Desert Research Institute, 2215 Raggio Parkway, Reno, NV 89512, USA. (rina@gbis.com)

M. M. Meerschaert, Department of Mathematics, University of Nevada, Reno, NV 89577-0084, USA.